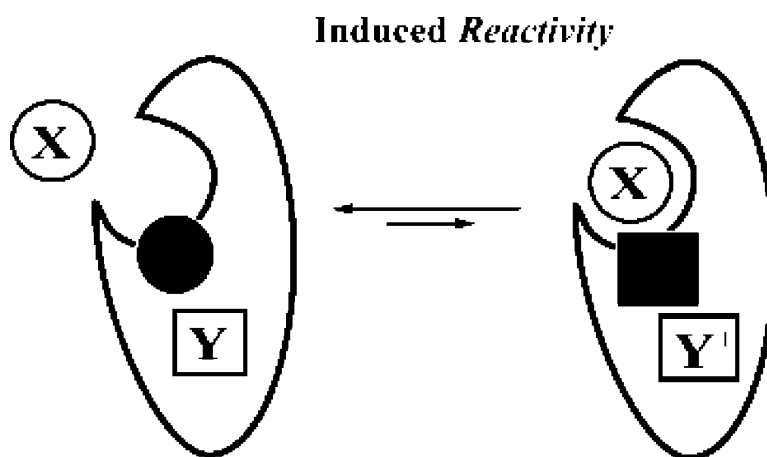


Substrate Modulation of the Properties and Reactivity of the Oxy-Ferrous and Hydroperoxo-Ferric Intermediates of Cytochrome P450cam As Shown by Cryoreduction-EPR/ENDOR Spectroscopy

Roman Davydov, Roshan Perera, Shengxi Jin, Tran-Chin Yang, Thomas A. Bryson, Masanori Sono, John H. Dawson, and Brian M. Hoffman

J. Am. Chem. Soc., **2005**, 127 (5), 1403-1413 • DOI: 10.1021/ja045351i • Publication Date (Web): 13 January 2005

Downloaded from <http://pubs.acs.org> on March 24, 2009



More About This Article

Additional resources and features associated with this article are available within the HTML version:

- Supporting Information
- Links to the 16 articles that cite this article, as of the time of this article download
- Access to high resolution figures
- Links to articles and content related to this article
- Copyright permission to reproduce figures and/or text from this article

[View the Full Text HTML](#)



Substrate Modulation of the Properties and Reactivity of the Oxy-Ferrous and Hydroperoxo-Ferric Intermediates of Cytochrome P450cam As Shown by Cryoreduction-EPR/ENDOR Spectroscopy

Roman Davydov,[†] Roshan Perera,[‡] Shengxi Jin,[‡] Tran-Chin Yang,[†]
Thomas A. Bryson,[‡] Masanori Sono,[‡] John H. Dawson,^{*,‡} and Brian M. Hoffman^{*,†}

Contribution from the Department of Chemistry, Northwestern University, Evanston, Illinois 60208, and Department of Chemistry and Biochemistry and School of Medicine, University of South Carolina, Columbia, South Carolina 29208

Received August 2, 2004; E-mail: bmh@northwestern.edu

Abstract: EPR/ENDOR studies have been carried out on oxyferrous cytochrome P450cam one-electron cryoreduced by γ -irradiation at 77 K in the absence of substrate and in the presence of a variety of substrates including its native hydroxylation substrate, camphor (**a**), and the alternate substrates, 5-methylenyl-camphor (**b**), 5,5-difluorocamphor (**c**), norcamphor (**d**), and adamantanone (**e**); the equivalent experiments have been performed on the T252A mutant complexed with **a** and **b**. The present study shows that the properties and reactivity of the oxyheme and of both the primary and the annealed intermediates are modulated by a bound substrate. This includes alterations in the properties of the heme center itself (**g** tensor; ¹⁴N, ¹H, hyperfine couplings). It also includes dramatic changes in reactivity: the presence of any substrate increases the lifetime of hydroperoxoferri-P450cam (**2**) no less than ca. 20-fold. Among the substrates, **b** stands out as having an exceptionally strong influence on the properties and reactivity of the P450cam intermediates, especially in the T252A mutant. The intermediate, **2**(T252A)-**b**, does not lose H₂O₂, as occurs with **2**(T252A)-**a**, but decays with formation of the epoxide of **b**. Thus, these observations show that substrate can modulate the properties of both the monooxygenase active-oxygen intermediates and the proton-delivery network that encompasses them.

The committed portion of the catalytic monooxygenation of substrate by cytochromes P450 and other dioxygen-activating heme enzymes^{1,2} begins with one-electron reduction of the [FeO₂]⁶ dioxygen-bound ferroheme,^{3,4,5} to generate an [FeO₂]⁷ intermediate assigned as a peroxoferriheme (**1**). Through cryoreduction EPR/ENDOR measurements, we recently confirmed that the hydroxylation of camphor by cytochrome P450cam involves the following steps: intermediate **1** converts to the hydroperoxoferri heme intermediate ([FeO₂H],⁷ **2**); this species accepts a second proton and undergoes heterolytic O—O cleavage to produce compound I (**3**), which is the catalytically active species, Scheme 1. However, it has been proposed that under appropriate circumstances, intermediates **1** and **2** can react with some substrates.^{6–8} Thus, the nucleophilic intermediate **1**

was shown to oxidize highly electrophilic substrates such as aldehydes;^{9–11} the electrophilic intermediate **2** was proposed to oxidize electron-rich double bonds and is the oxidant in reactions catalyzed by heme oxygenase.^{12–14} We thus are led to ask: how do an enzyme and its substrate choose the reactive intermediate?

Much attention has been given to the role of the enzyme active-site environment,^{1,15–19} so beautifully revealed for P450cam

[†] Northwestern University.

[‡] University of South Carolina.

- (1) Sono, M.; Roach, M. P.; Coulter, E. D.; Dawson, J. H. *Chem. Rev.* **1996**, *96*, 2841–2887.
- (2) Ortiz de Montellano, P. R., Ed. *Cytochrome P450*, 2nd ed.; Plenum Press: New York, 1995.
- (3) Here, $n = 6$ is the sum of the number of electrons in 3d orbitals on Fe and in antibonding orbitals on oxygen.
- (4) Westcott, B. L.; Enemark, J. H. *Inorg. Electron. Struct. Spectrosc.* **1999**, *2*, 403–450.
- (5) Davydov, R.; Satterlee, J. D.; Fujii, H.; Sauer-Masarwa, A.; Busch, D. H.; Hoffman, B. M. *J. Am. Chem. Soc.* **2003**, *125*, 16340–16346.
- (6) Coon, M. J.; Vaz, A. D. N.; McGinnity, D. F.; Peng, H.-M. *Drug Metab. Dispos.* **1998**, *26*, 1190–1193.

- (7) Newcomb, M.; Shen, R.; Choi, S.-Y.; Toy, P. H.; Hollenberg, P. F.; Vaz, A. D. N.; Coon, M. J. *J. Am. Chem. Soc.* **2000**, *122*, 2677–2686.
- (8) Jin, S.; Makris, T. M.; Bryson, T. A.; Sligar, S. G.; Dawson, J. H. *J. Am. Chem. Soc.* **2003**, *125*, 3406–3407.
- (9) Fischer, R. T.; Trzaskos, J. M.; Magolda, R. L.; Ko, S. S.; Brosz, C. S.; Larsen, B. *J. Biol. Chem.* **1991**, *266*, 6124–6132.
- (10) Akhtar, M.; Corina, D.; Miller, S.; Shyadehi, A. Z.; Wright, J. N. *Biochemistry* **1994**, *33*, 4410–4418.
- (11) Ortiz de Montellano, P. R.; De Voss, J. *J. Nat. Prod. Rep.* **2002**, *19*, 477–493.
- (12) Ortiz de Montellano, P. R. *Acc. Chem. Res.* **1998**, *31*, 543–549.
- (13) Davydov, R.; Kofman, V.; Fujii, H.; Yoshida, T.; Ikeda-Saito, M.; Hoffman, B. M. *J. Am. Chem. Soc.* **2002**, *124*, 1798–1808.
- (14) Davydov, R.; Matsui, T.; Fujii, H.; Ikeda-Saito, M.; Hoffman, B. M. *J. Am. Chem. Soc.* **2003**, *125*, 16208–16209.
- (15) Gerber, N. C.; Sligar, S. G. *J. Am. Chem. Soc.* **1992**, *114*, 8742–8743.
- (16) Schlichting, I.; Berendzen, J.; Chu, K.; Stock, A. M.; Maves, S. A.; Benson, D. E.; Sweet, B. M.; Ringe, D.; Petsko, G. A.; Sligar, S. G. *Science* **2000**, *287*, 1615–1622.
- (17) Davydov, R.; Makris, T. M.; Kofman, V.; Werst, D. W.; Sligar, S. G.; Hoffman, B. M. *J. Am. Chem. Soc.* **2001**, *123*, 1403–1415.
- (18) Harris, D. L.; Loew, G. H. *J. Am. Chem. Soc.* **1998**, *120*, 8941–8948.
- (19) Guallar, V.; Baik, M.-H.; Lippard, S. J.; Friesner, R. A. *Proc. Natl. Acad. Sci. U.S.A.* **2003**, *100*, 6998–7002.

Scheme 1

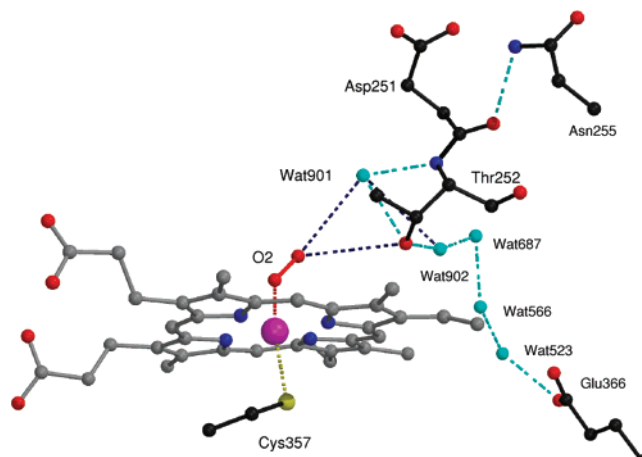
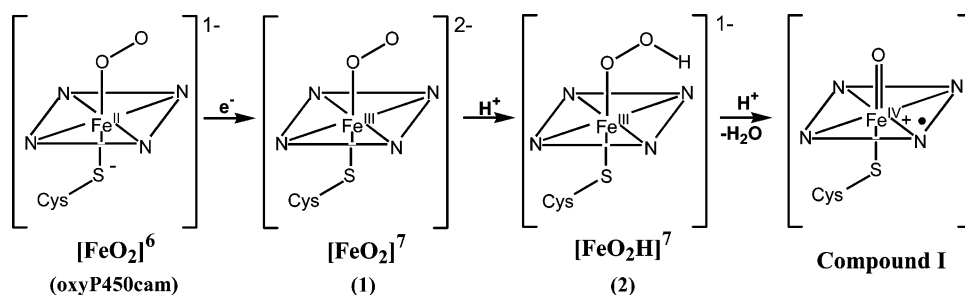
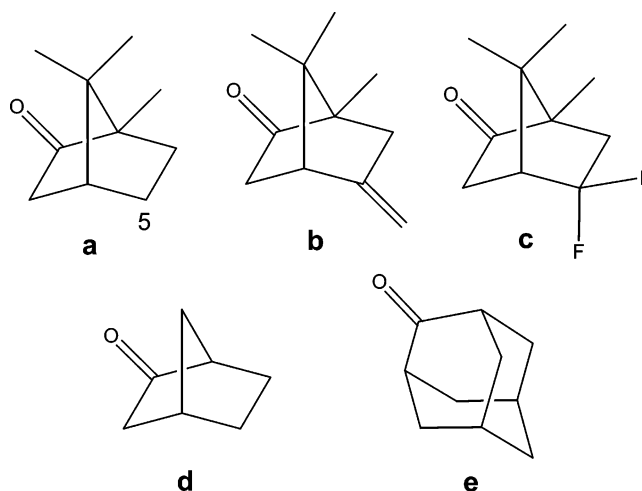


Figure 1. Structure of the active site of oxyferrous-P450cam as adopted from the paper of Schlichting et al.¹⁶

in the crystal structure of the camphor complex of the oxyferrous state, Figure 1,¹⁶ a perspective that implicitly assumes that the substrate plays a passive role: intermediates become increasingly reactive in the progression, **1** \rightarrow **3**, and the first intermediate generated that is thermodynamically and kinetically competent is the one that reacts. However, there is considerable evidence that the presence of substrate in the heme pocket can modify the structure and reactivity of the enzyme active site in the early stages of the monooxygenase catalytic cycle—the ferric, ferrous, and oxy-ferrous states. As examples, it is known that the stability²⁰ and MCD spectra of oxyferrous cytochrome-P450 are strongly influenced by the presence of substrate.^{21–23} Binding of substrates causes expulsion of water coordinated to the heme iron(III) of P450cam and changes its potential,^{1,2,11,24} changes the rate constant for CO binding to ferrous P450^{20,23,25} and the CO stretching frequency,^{26,27} increases the stability of the oxyferrous complex toward autoxidation,²⁰ and influences the resonance Raman (RR) spectra of ferrous P450cam-NO.²¹

The present studies address the question: can the substrate modulate the properties and reactivity of intermediates in the later, reactive, stages of the monooxygenase reaction cycle?

Chart 1



Cryoreduction-EPR/ENDOR studies^{13,17,28} have been carried out on the intermediates formed when oxyferrous-P450cam and its T252A mutant, both substrate-free (WT) and complexed with substrates **a–e** (Chart 1), are subjected to 77 K cryoreduction and subsequent annealing. These demonstrate that changes in substrate can alter the properties of oxyferrous-P450cam and can influence the steps in the monooxygenase reaction cycle that follow its reduction, at least through the reaction of the hydroperoxy-ferric-P450cam intermediate. They thus show that under appropriate circumstances, the substrate can play a previously undetected active role in modulating the properties and reactivity of active-oxygen intermediates in the catalytic cycle of cytochrome P450.

Experimental Procedures

Materials. Solid $\text{Na}_2\text{S}_2\text{O}_4$, ethylene glycol, (1R) camphor, (1S) camphor, norcamphor, adamantanone, and all other reagents were purchased from standard commercial sources and used as received. O_2 and CO gases were obtained from Matheson Co. The syntheses of (1R)-5,5-difluorocamphor (5-F₂-camphor),²⁹ and (1R) methylenecamphor³⁰ were carried out as previously reported.

Sample Preparations. Recombinant wild-type and T252A mutant P450-CAM proteins were expressed in *Escherichia coli* and purified as reported^{31–34} and kept frozen at -80°C at 50–100 μM concentra-

(20) Eisenstein, L.; Debey, P.; Douzou, P. *Biochem. Biophys. Res. Comm.* **1977**, *77*, 1377–1383.

(21) Hu, S.; Kincaid, J. R. *J. Am. Chem. Soc.* **1991**, *113*, 9760–9766.

(22) Sono, M.; Perera, R.; Jin, S.; Makris, T. M.; Sligar, S. G.; Bryson, T. A.; Dawson, J. H. *Arch. Biochem. Biophys.*, in press.

(23) Lipscomb, J. D.; Sligar, S. G.; Namtvedt, M. J.; Gunsalus, I. C. *J. Biol. Chem.* **1976**, *251*, 1116–1124.

(24) Sligar, S. G.; Gunsalus, I. C. *Proc. Natl. Acad. Sci. U.S.A.* **1976**, *73*, 1078–1082.

(25) Unno, M.; Ishimori, K.; Ishimura, Y.; Morishima, I. *Biochemistry* **1994**, *33*, 9762–9768.

(26) Schulze, H.; Ristau, O.; Jung, C. *Eur. J. Biochem.* **1994**, *224*, 1047–1055.

(27) Jung, C.; Ristau, O.; Schulze, H.; Sligar, S. G. *Eur. J. Biochem.* **1996**, *235*, 660–669.

(28) Davydov, R.; Ledbetter-Rogers, A.; Martasek, P.; Larukhin, M.; Sono, M.; Dawson, J. H.; Masters, B. S. S.; Hoffman, B. M. *Biochemistry* **2002**, *41*, 10375–10381.

(29) Eble, K. S.; Dawson, J. H. *J. Biol. Chem.* **1984**, *259*, 14389–14393.

(30) Maryniak, D. M.; Kadkhodayan, S.; Crull, G. B.; Bryson, T. A.; Dawson, J. H. *Tetrahedron* **1993**, *49*, 9373–9384.

(31) Martinis, S. A.; Atkins, W. M.; Stayton, P. S.; Sligar, S. G. *J. Am. Chem. Soc.* **1989**, *111*, 9252–9253.

(32) Gunsalus, I. C.; Wagner, G. C. *Methods Enzymol.* **1978**, *52*, 166–188.

(33) O'Keefe, D. H.; Ebel, R. E.; Peterson, J. A. *Methods Enzymol.* **1978**, *52*, 151–157.

tions in 100 mM potassium phosphate buffer (pH 7.5) containing 1 mM camphor. EPR/ENDOR samples of oxyferrous complexes were prepared from ferric wild-type P450cam (0.6–1.0 mM) and T252A P450cam (0.6–1.0 mM) mutant in a cryosolvent: ethylene glycol/100 mM potassium phosphate buffer (pH 8.0 for H₂O buffer and pH 7.5 for D₂O buffer), using both [40:60] and [60:40] v/v solutions with no significant distinction. Kinetic measurements used 40:60 (v/v) ethylene glycol/buffer to prevent bubble formation during a kinetic measurement; EPR measurements on camphor-free ferric P450-CAM were prepared by first removing the (1*R*) camphor³³ from wild-type P450cam or its T252A mutant. The P450 samples with other camphor derivatives bound were prepared by adding the respective camphor analogues from stock solutions (100 mM in ethylene glycol) to the camphor-free protein. Final concentrations for each camphor analogue were as follows: (1*R*) camphor (2–3 mM), norcamphor (~10 mM), adamantanone (~4 mM), (1*R*)-5,5-difluorocamphor (2–3 mM), and (1*R*) methylenylcamphor (10–15 mM). The reduced protein samples were prepared from the corresponding ferric samples by microliter additions of a near minimal amount of Na₂S₂O₄ (up to 0.35 mM from a 20 mg/mL buffer) under nitrogen atmosphere at 4 °C. Ferrous-O₂ complexes were generated at ~-40 °C in a chest freezer box in a mixed cryosolvent [ethylene glycol/100 mM potassium phosphate buffer (pH 8.0 for H₂O buffer and pH 7.5 for D₂O buffer) (40:60 v/v)] gently bubbled with cold oxygen to dithionite-reduced protein.

Measurements. Cryoreduction/annealing protocols and 35 GHz CW EPR/ENDOR procedures have been described.^{13,17,28} For a single orientation of a paramagnetic center, the first-order ENDOR spectrum of a nucleus with $I = 1/2$ in a single paramagnetic center consists of a doublet with frequencies given by³⁵

$$\nu_{\pm} = |\nu_N \pm A/2| \quad (1)$$

Here, ν_N is the nuclear Larmor frequency and A is the orientation-dependent hyperfine coupling constant of the coupled nucleus. The doublet is centered at the Larmor frequency and separated by A when $\nu_N > |A/2|$, as in the case for ¹H spectra presented here. For ¹⁴N ($I = 1$), a single orientation gives a four-line pattern

$$\nu_{\pm}(\pm) = |\nu_N \pm A/2| \pm 3P/2 \quad (2)$$

in which both ν_+ and ν_- branches, described by eq 1, are farther split into a doublet by the quadrupole splitting, $3P$. For the heme pyrrole ¹⁴N studied here, only the ν_+ branch is readily observed in spectra collected at 35 GHz. As an illustration, Figure 2 presents a ¹⁴N ENDOR spectrum taken at g_1 of **2-b** (discussed in detail next); the brackets illustrate an assignment as overlapping ν_+ doublets (eq 2) from two distinct types of pyrrole ¹⁴N. The full hyperfine and quadrupole tensors of the coupled nucleus can be obtained by analyzing a 2-D field-frequency set of orientation-selective ENDOR spectra across the EPR envelope, as described elsewhere.^{36–38}

Results

States Produced by Cryoreduction/Annealing. (1) P450cam. Substrate-Free. As a reference point from which to assess how the substrate can modulate the properties of hydroperoxo-ferric-P450cam (**2**), we cryoreduced substrate-free oxyferrous-P450cam by γ -irradiating ethylene glycol/buffer glassy solutions of oxyferrous-P450cam frozen at 77 K. Although autoxidation

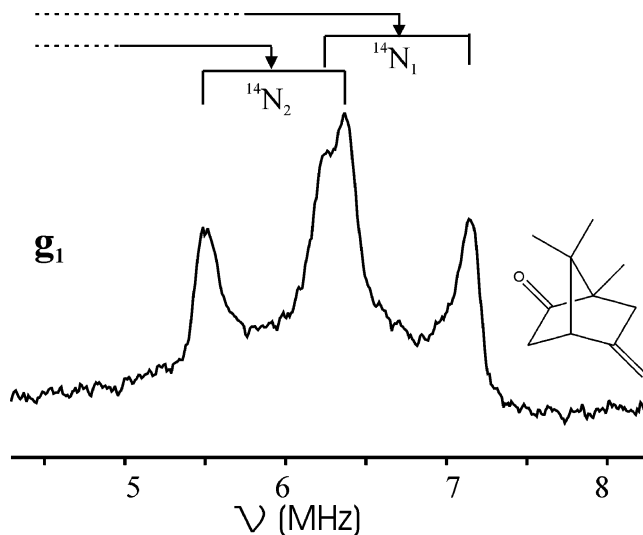


Figure 2. CW 35 GHz ¹⁴N g_1 ENDOR spectrum of **2-b** after being annealed at 170 K for 1 min. Brackets indicate assignments to the ν_+ doublets (eq 2) from two types of ¹⁴N. Conditions: modulation frequency 100 kHz, modulation amplitude 1.5 G, microwave frequency 35 GHz, microwave power 35 db, sweep rate 0.2 MHz/s, RF power 20 W, RF broadening 25 KHz, and $T = 2$ K. Data for all figures were collected from samples prepared in ethylene glycol/buffer as described in the Experimental Procedures.

to low-spin ferri-P450cam during oxygenation prior to cryoreduction was substantial, the EPR spectrum of irradiated frozen oxyferrous-P450cam (Figure 3) clearly shows the presence of the hydroperoxo intermediate, **2**. The majority form of **2** exhibits an unusually anisotropic g tensor ($g_1 = 2.355$; Table 1), as does **2** in heme oxygenase,¹³ which has the heme itself as substrate and thus also has no additional organic substrate bound. A minor form of **2** has a g tensor typical of most hydroperoxo ferriheme species studied ($g_1 = 2.30$; Table 1).

¹H ENDOR spectra of **2** taken at multiple fields show a signal from the hydroperoxo proton, with maximum hyperfine coupling $A_{\max} = 9.9$ MHz and $A(g_1) = 8.8$ for the majority form (Table 1). The ν_+ branch of the ¹⁴N spectrum of **2** (majority) taken at g_1 (Figure 4) is dominated by two quadrupole-split doublets, eq 2 ($Q_1 = 1.1$ MHz, $A_1 = 5.38$ MHz; $Q_2 = 1$ MHz, $A_2 = 7.08$ MHz), quite similar to that of Figure 2. Such a spectrum might arise from two enzyme substates, each with four equivalent pyrrole ¹⁴N, but most likely¹⁷ is from a single substate with 2-fold effective symmetry at Fe and hence two types of pyrrole ¹⁴N. Other weaker features in the spectrum arise from the underlying EPR spectra of other ferriheme species.

Upon **2** being annealed to temperatures below 170 K, the two forms relax with small changes in g values (Figure 3), which nonetheless leave g_1 unusually large for the majority form, Table 2. The EPR signal of **2** in fact slowly disappears during annealing at these temperatures, but nonetheless, we were able to measure the ¹H and ¹⁴N ENDOR spectra of **2** (majority) after relaxation. The hyperfine coupling to the hydroperoxo proton remains about the same (Table 2), and the basic features of the ¹⁴N ENDOR spectrum are unchanged (Figure 4), with only slight shifts in the spin-Hamiltonian parameters of the pyrrole ¹⁴N. The hydroperoxo intermediate completely disappeared during annealing at 180 K for 1 min.

Camphor (a). Cryoreduction of the oxyferrous-P450cam-a complex in EG-buffer glass at 77 K yields comparable amounts of ferriheme species **1-a** and **2-a** (Figure 3), with the g tensors

(34) Raag, R.; Martinis, S. A.; Sliagar, S. G.; Poulos, T. L. *Biochemistry* **1991**, *30*, 11420–11429.

(35) Abragam, A.; Bleaney, B. *Electron Paramagnetic Resonance of Transition Metal Ions*, 2nd ed.; Clarendon Press: Oxford, 1970.

(36) Hoffman, B. M.; Gurbiel, R. J.; Werst, M. M.; Sivaraja, M. In *Advanced EPR. Applications in Biology and Biochemistry*; Hoff, A. J., Ed.; Elsevier: Amsterdam, 1989; pp 541–591.

(37) Hoffman, B. M. *Acc. Chem. Res.* **1991**, *24*, 164–170.

(38) Hoffman, B. M.; DeRose, V. J.; Doan, P. E.; Gurbiel, R. J.; Houseman, A. L. P.; Telsler, J. *Biol. Magn. Reson.* **1993**, *13* (EMR of Paramagnetic Molecules), 151–218.

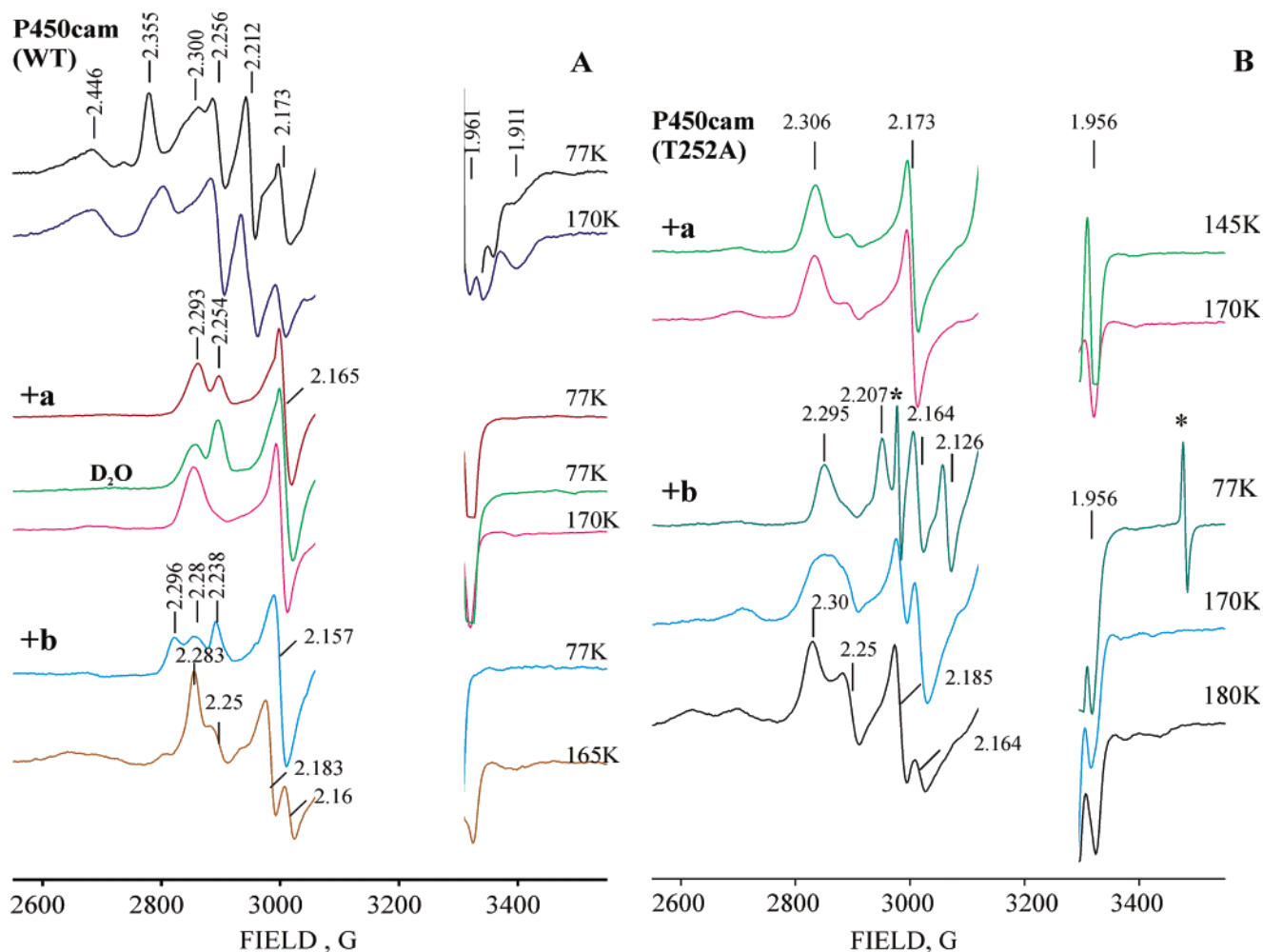


Figure 3. X-band EPR spectra of oxyferrous-P450cam and oxyferrous-P450cam(T252A) cryoreduced at 77 K. (A) Oxyferrous-P450cam without substrate and in the presence of **a** and **b**; as reduced at 77 K and after annealing at indicated temperatures. D₂O means D₂O/40% *d*₂-EG buffer. (B) Oxyferrous-P450cam(T252A) P450 with **a** and **b**; as reduced at 77 K and after being annealed at indicated temperatures. Asterisks represent H-atom doublet. Conditions: 100 kHz modulation amplitude 5 G, microwave power 20 mW, microwave frequency 9.100 GHz, and $T = 77$ K.

Table 1. EPR and ¹H ENDOR Parameters for Primary Species of Cryoreduced Oxyferrous-P450^a

substrate	species	WT					T252 A					
		g_1	g_2	g_3	$A(g_1)$	A_{\max}	g_1	g_2	g_3	$A(g_1)$	A_{\max}	
substrate-free	2	2.355	2.212	1.935	8.8	9.9						
	2(minor)	2.30	2.173	nd								
camphor (a) ^b	2	2.289	2.165	1.956	10	11.2	2	2.306	2.173	1.956	8.5	11.5
	1	2.254	2.165	1.956								
5-methylenyl camphor (b) ^b	2	2.296	2.157	1.957	8.5	11.6	2	2.295	2.164	~1.96	8.3	12.3
	1	2.28	2.157	1.957			1	2.207	2.126	nd		
5-F ₂ camphor (c) ^b	2	2.238	2.157	nd								
	1	2.302	2.174	nd	8.0	13.6						
norcamphor (d)	2	2.262	2.174	nd								
	1	2.288	2.157	~1.96	12.4	14.3						
adamantanone (e)	2	2.30	2.162	~1.96	8.5	11.5						
	1	2.257	2.16	nd								

^a Prepared in ethylene-glycol buffer as described in the Experimental Procedures. ^b The relative proportions of the species changes in D₂O buffer. ^c $A = [5, 7, 11]$ MHz; $\varphi = 50^\circ$, $\theta = 90^\circ$; $\psi = 50^\circ$ (Euler angles). ^d $A = [5, 7.5, 1]$ MHz; $\varphi = 30^\circ$, $\theta = 70^\circ$; $\psi = 35^\circ$ (Euler angles).

given in Table 1. Interestingly, the relative population of species **2-a** is substantially less with D₂O/*d*₂-EG as solvent (Figure 2). With 20% glycerol solutions, the primary product of 77 K cryoreduction was shown to be largely **2-a**; observation of **1-a** required cryoreduction at helium temperatures;¹⁷ however, the g values of **2-a** are the same as those of **2-a** in 20% glycerol. Proton ENDOR spectra of **2-a**, in EG/buffer taken at fields where signals from **1-a** and **2-a** do not overlap, show that the

hydroperoxo proton of **2-a** has a hyperfine coupling at g_1 of $A(g_1) = 10$ MHz (Table 1), the same as for the sample in glycerol/buffer.

Annealing the cryoreduced EG-buffer sample for 1 min at 170 K causes complete conversion to **2-a** (Figure 3), whose g tensor has changed very little (Table 2). Proton ENDOR spectra of the hydroperoxo proton(s) of relaxed **2-a** were collected at multiple fields across the EPR envelope. They produce a 2-D

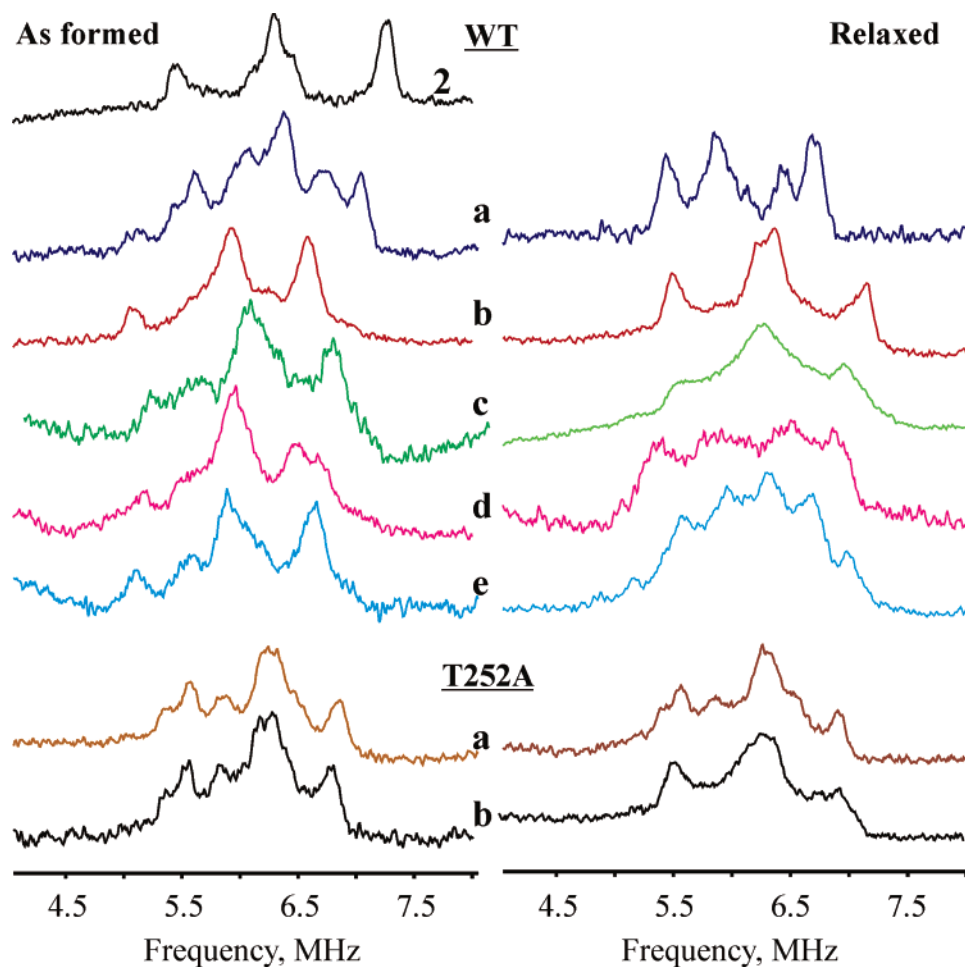


Figure 4. CW 35 GHz ^{14}N ENDOR spectra taken at g_1 of hydroperoxo intermediates generated by cryoreduction of substrate (a–e) complexes of oxyferrous-P450cam and oxyferrous-P450cam(T252A): (left) as formed and (right) after being annealed at 170 K for 1 min. Conditions: modulation frequency 100 kHz, modulation amplitude 1.5 G, microwave frequency 35 GHz, microwave power 35 db, sweep rate 0.2 MHz/s, RF power 20 W, RF broadening 25 KHz, and $T = 2$ K.

Table 2. EPR and ^1H ENDOR Parameters for Relaxed Hydroperoxoferri P450Cam Species^a

substrate	WT					T252 A				
	g_1	g_2	g_3	$A(g_1)$	A_{max}	g_1	g_2	g_3	$A(g_1)$	A_{max}
substrate-free ^b	2.34	2.215	1.94	8.8	10					
camphor (a)	2.293	2.17	1.956	8.0 ^c	11.5 ^c	2.306	2.173	1.956	8.5	11.5
5-methylenyl camphor (b)	2.283	2.183	1.96	6.2 ^d	7.5 ^d	~2.30	2.185	~1.96	8.8	10.6
5-F ₂ camphor (c)	2.311	2.195	~1.96	~9	~9	~2.30	2.164	~1.96		
	2.294	2.18	~1.96							
	2.343	2.17	1.958							
norcamphor (d) ^a	2.29	2.156	1.959	8.0	11.2					
adamantanone (e) ^a	2.288	2.166	1.958	11.2	11.2					

^a Prepared in ethylene-glycol buffer as described in the Experimental Procedures. ^b Trace amounts of species with slightly different g tensors also appear during relaxation. ^c $\mathbf{A} = [5, 7, 11]$ MHz; $\varphi = 50^\circ$, $\theta = 90^\circ$ m; $\psi = 50^\circ$ (Euler angles). ^d $\mathbf{A} = [5, 7.5, 1]$ MHz; $\varphi = 30^\circ$, $\theta = 70^\circ$ m; $\psi = 35^\circ$ (Euler angles).

field-frequency pattern (Figure 5) that is well-described by a hyperfine tensor (Table 2) that matches the one reported previously;¹⁷ values of A_{max} and $A(g_1)$ are listed for comparison with those for species where full tensors could not be derived.

The ^{14}N ENDOR spectrum taken at g_1 of **2-a** as formed by cryoreduction differs significantly from that of **2** (Figure 4). It is quite complicated, with at least seven features in the ν_+ branch, which requires at least four types of ^{14}N (eq 2). Although such a spectrum could arise from a single enzyme substrate whose unsymmetrical heme has four inequivalent pyrrole ^{14}N , almost certainly it arises from two or more substates. Annealing to 170 K for 1 min allows the as-formed **2-a** to undergo

structural relaxation. The ^{14}N ENDOR spectrum of relaxed **2-a** remains complicated (Figure 4) but is sharpened and exhibits six features that can be assigned to three distinct ^{14}N whose hyperfine and quadrupole couplings differ from those of the initial product of cryoreduction; again, the spectrum likely comes from two substates with three distinct ^{14}N between them; hyperfine and quadrupole couplings are listed in Table S1.

Extended annealing of **2-a** at 180 K causes its conversion to the primary product state (Figure 6; $\mathbf{g} = [2.62, 2.18, 1.865]$), in which the hydroxyl of the stereospecifically formed 5-exo-hydroxy-camphor enzymatic product is bound to the ferriheme in a nonequilibrium conformation.¹⁷ In the present experiments

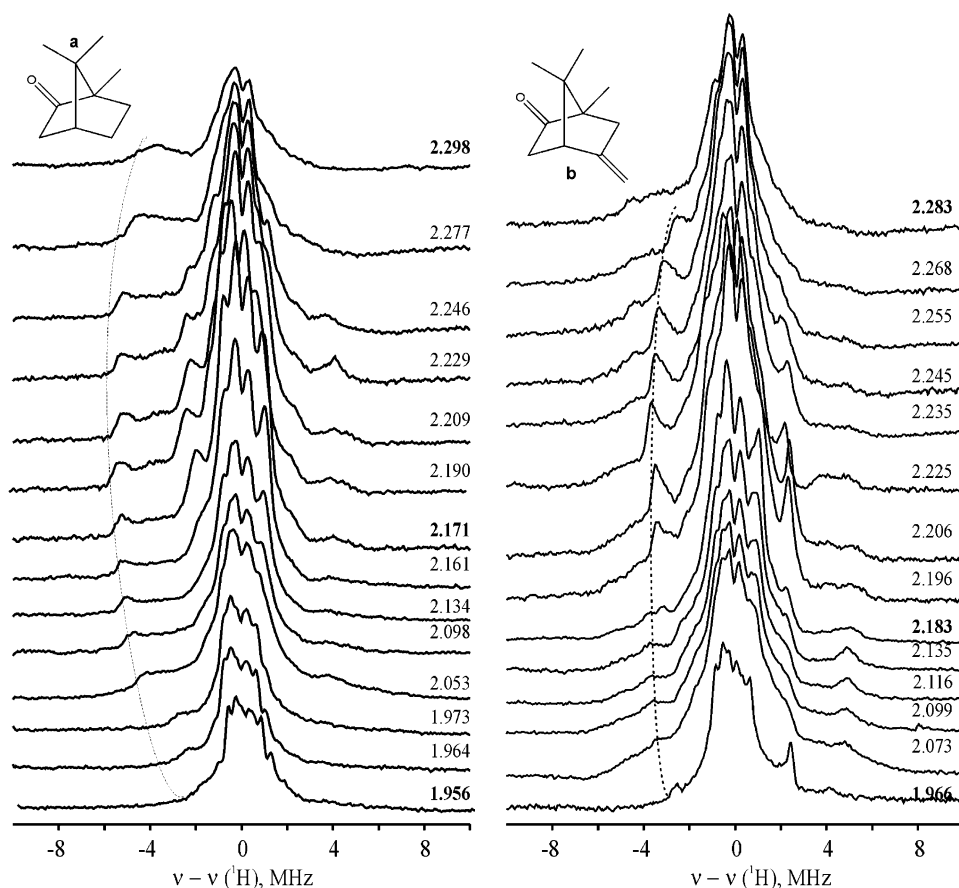


Figure 5. Orientation-selective, 2-D field/frequency ^1H CW 35 GHz ENDOR patterns for complexes of oxyferrous-P450cam complexes **a** and **b** cryoreduced at 77 K and annealed for 1 min at 171 and 165 K, respectively. Conditions: modulation frequency 100 kHz, modulation amplitude 1.5 G, microwave frequency 35 GHz, microwave power 35 db, sweep rate 0.5 MHz/s, RF power 10 W, RF broadening 60 kHz, and $T = 2$ K.

with EG/buffer as solvent, some of the **2-a** intermediate converts directly to the equilibrium form of product-bound ferri P450cam (Figure 6; $g = (2.48, 2.26, 1.91)$), which was not the case with cryoreduced oxyferrous-P450cam(D251N) in glycerol/buffer glass;¹⁷ in addition, other low- and high-spin forms of ferric P450 also are generated.

5-Methylenyl-camphor (b). EPR spectra generated by cryoreduction of the oxyferrous-P450cam-**b** complex at 77 K exhibit a signal from **1-b**, which has a different g tensor from that of **1-a** (Figure 3); they also show signals from two forms of **2-b**, both with g tensors different from that of **2-a** (Table 1). As with oxyP450cam-**a**, the relative amount of **2-b** generated decreases with deuterated solvent (not shown). Upon the sample being annealed for 1 min at $\sim 165\text{K}$, the as-formed **1-b** and **2-b** relax to a single **2-b** form (Figure 3) whose g tensor components (Table 2) differ from those of **2-a** (Table 2). The EPR signal of this **2-b** intermediate also is sharper than that of relaxed **2-a**, unexpectedly indicating a better-defined structure for the relaxed $[\text{FeO}_2\text{H}]^7$ state complexed with the alternate substrate (Figure 3). Indeed, this spectrum is sharper than that of any other substrate complex of **2**.

The ENDOR-derived g_1 hyperfine couplings of the hydroperoxo proton in as-formed **2-b** are similar to those of as-formed **2-a** (Table 1) (overlap of the **2-b** EPR spectrum with that of **1-b** precludes determination of the full hyperfine tensor). The hydroperoxo proton hyperfine couplings ($A(g_1)$ and A_{max}) for relaxed **2-b** formed during annealing at 165 K are notably smaller than those of all other **2** species studied (Table 2). This

difference is quite apparent in the 2-D field-frequency plots of relaxed **2-a** and **2-b** (Figure 5) and in the differing hyperfine tensors that describe these two plots (Table 2).

The ν_+ branch of the $g_1 = 2.296$ ^{14}N spectrum of as-formed **2-b** is simpler than that of **2-a** and rather like that of **2** (Figure 3); it is dominated by one sharp quadrupole-split doublet, with weaker features that can be assigned to two other doublets. Upon relaxation during 1 min of annealing at 165 K, the ^{14}N spectrum of **2-b** further sharpens and is cleanly assignable to two types of ^{14}N with hyperfine/quadrupole couplings that have changed appreciably upon relaxation ($Q_1 = 0.84$ MHz, $A_1 = 5.1$ MHz; $Q_2 = 0.88$ MHz, $A_2 = 6.7$ MHz). Thus, the ^{14}N ENDOR spectra of the relaxed **2-a**, and **2-b** differ notably from each other in the number of observed peaks/distinct ^{14}N and in their corresponding spin-Hamiltonian parameters. The ^{14}N spectrum of relaxed **2-b** in fact is the cleanest of those from any yet seen for a substrate complex of **2** and **2(T252A)** (Figures 2 and 4).

During further annealing at 180 K, **2-b** decays to a ferriheme state with $g = [2.47, 2.26, 1.934]$ and then on to what appears to be an aquoferriheme state with $g_1 = [2.43, 2.25, 1.91]$. GC-MS analysis shows that this decay is accompanied by stereospecific epoxidation of **b** with no less than $\sim 25\%$ of total enzyme forming product, in agreement with results at ambient temperatures.³⁹ As $\sim 80\%$ of enzyme is frozen in the oxyferrous state, and no more than 50% of that is cryoreduced, it appears that no less than 50% of **2-b** forms product. It is noteworthy that

(39) Kadkhodayan, S.; Coulter, E. D.; Maryniak, D. M.; Bryson, T. A.; Dawson, J. H. *J. Biol. Chem.* **1995**, *270*, 28042–28048.

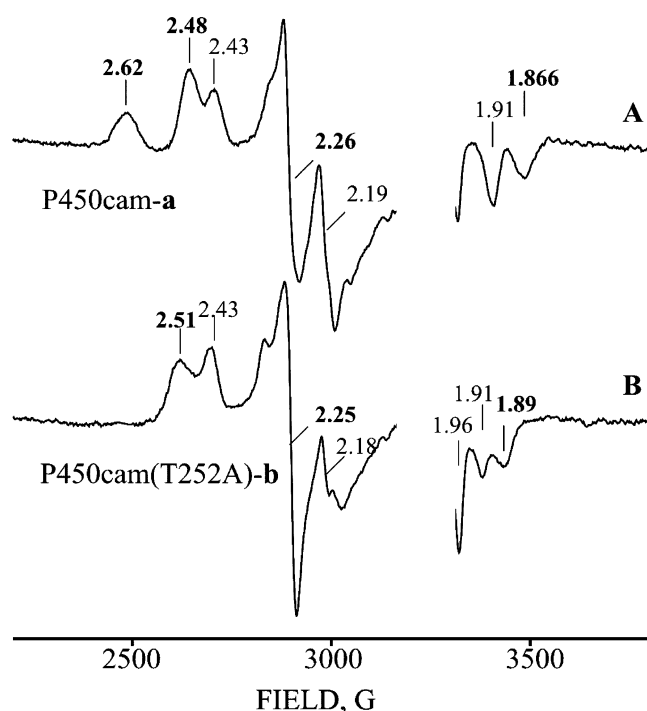


Figure 6. EPR spectra of cryoreduced oxyferrous-P450cam-**a** and oxyferrous-P450cam(T252A)-**b** annealed at 180 K for 50 and 1200 min, respectively. Conditions: as in Figure 3.

proton ENDOR spectra of the $g_1 = 2.47$ ferriheme state show no strongly coupled protons ($A(g_1) \leq 5$ MHz). A possible interpretation of this finding is that the $g_1 = 2.47$ state is the nonequilibrium complex of the epoxide product that forms upon epoxidation of **b** by compound I, analogous to the complex of hydroxycamphor that forms upon camphor hydroxylation.¹⁷

5-F₂-Camphor (c). Cryoreduction of oxyferrous-P450cam-**c** at 77 K is like the reduction of the **a** complex in that it yields comparable amounts of peroxo- and hydroperoxo ferriheme species **1-c** and **2-c**, although with slightly altered **g** tensors from those of **1-a** and **2-a** (Table 1); the relative amount of **2-c** also decreases with deuterated solvent. The maximum hydroperoxo proton coupling for **2-c** as initially formed is larger than that for **2-a** (Table 1); the ν_+ branch of the g_1 ¹⁴N ENDOR spectrum of **2-c** is complicated, like that of **2-a**, but is less well-resolved (Figure 4).

The as-formed **1-c** and **2-c** show more complex relaxation behavior during annealing than do the corresponding intermediates of oxyferrous-P450cam complexed with **a** or **b**. At ~160 K, the as-formed **1-c** and **2-c** convert to three new spectroscopically distinct forms of **2-c** (Table 2; Figure 3). Upon subsequent annealing at 180 K, these convert to high- and low-spin ferric forms of ferri-P450cam; there are two of the latter, $\mathbf{g} = [2.46, 2.25, 1.91]$ and $\mathbf{g} = [2.43, 2.17, 1.93]$, the second at least being assignable to aquo-ferri P450cam. As reaction in the presence of **c** largely leads to uncoupled formation of water, and relatively little of the 9-OH-**c** product,³⁹ observation of a product complex is not expected.

The g_1 ¹⁴N (Figure 4) and ¹H (not shown) ENDOR spectra of as-formed **2-c** also are like those of **2-a**: the ¹⁴N spectrum is complicated; the proton spectrum has $A_{\max} \sim 13.6$ MHz. Relaxation at ~170 K decreases A_{\max} to ~10.5 MHz and simplifies the $\mathbf{g} = 2.29$ N ENDOR spectrum (Figure 4).

Norcamphor (d). Cryoreduction of oxyferrous-P450cam-**d** generates a single form of **2-d** with $g_1 = 2.288$ (Table 1) and a hydroperoxy proton with $A_{\max} = 14.3$ MHz, noticeably bigger than that of **2-a**. The g_1 ¹⁴N ENDOR spectrum of **2-d** is complicated, like that of **2-a**, while differing from it in detail (Figure 4). Annealing the as-formed **2-d** at 170 K for 1 min causes a decrease in the intensity of the signal from the primary **2-d** species and a noticeable decrease of $A(g_1)$ and A_{\max} for the hydroperoxy proton (Tables 1 and 2) but little change in the **g** tensor (Table 2).

Adamantanone (e). Cryoreduction of oxyferrous-P450cam-**e** produces **1-e** and **2-e** with **g** tensors (Table 1) that are slightly different from these for hydroperoxo and peroxo species generated in the presence of substrates **a-d**. Annealing the cryoreduced sample at 145 K for 1 min converts **1-e** to **2-e**; an additional minute of annealing at 180 K causes small changes in the **g** tensor of **2-e**; prolonged annealing at 180 K causes the loss of **2-e** with concomitant formation of ferric P450cam in low- and high-spin states.

The hydroperoxy proton of the as-formed **2-e** has $A(g_1) = 8.5$ MHz and $A_{\max} \sim 11.5$ MHz, values comparable to those of the camphor complex; relaxation at 165 K increases $A(g_1)$ to 11.2 MHz without changing A_{\max} (Tables 1 and 2), which indicates a reorientation of the OOH moiety. The ν_+ branch of the ¹⁴N ENDOR spectrum of as-formed **2-e** taken at $g_1 = 2.3$ most resembles that of **2-c**; it shows four broadened features (Figure 4) that can be assigned two nonequivalent pairs of pyrrole nitrogens of low-spin ferriheme (see Table S1). When **2-e** relaxes at 165 K, it shows a more complex g_1 ¹⁴N ENDOR spectrum, consisting of six features (Figure 4).

(2) P450cam(T252A). Camphor. EPR spectra collected upon 77 K irradiation of oxyferrous-P450cam(T252A)-**a** show that **2(T252A)-a** is the primary cryoreduction product (Figure 3). Its **g** tensor differs noticeably from that of **2-a** (Table 1); as with **2-a**, the **g** tensor does not change upon relaxation at 180 K (Figure 3). The hyperfine interaction of the hydroperoxo proton of **2(T252A)-a** is similar to that of **2-a**, with $A_{\max} \sim 11.5$ MHz, in both the as-formed center and after relaxation (Tables 1 and 2). Likewise, the g_1 ¹⁴N ENDOR spectra of **2(T252A)-a**, both as initially formed by cryoreduction and after relaxation at 170 K, are qualitatively similar to the complicated spectra of **2-a** (Figure 4).

5-Methylenyl-camphor. Cryoreduction of oxyferrous-P450cam(T252A)-**b** at 77 K produces **1(T252A)-b** and **2(T252A)-b** with roughly equal EPR intensities (Figure 3); the relative amount of **2(T252A)-b** again decreases in deuterated solvent (not shown). The spectrum of **1(T252A)-b** has a low value of g_1 , approximately that seen when oxyferrous-Mb is cryoreduced⁴⁰ (Table 1); the **g** tensor of **2(T252A)-b** is comparable to that of the corresponding state of the WT enzyme, but the spectrum of the mutant is somewhat sharper (Figure 3). The as-formed **1(T252A)-b** converts to **2(T252A)-b** upon being annealed at 145 K; the rate of this conversion decreases noticeably in D₂O/*d*₂-EG. Further annealing to 180 K causes a slight change in g_2 of **2(T252A)-b** (Tables 1 and 2).

The maximum hyperfine coupling to the hydroperoxy proton of as-formed **2(T252A)-b** (Figure 5) is somewhat larger than that for initially formed **2-a, b** although the 2-D patterns are

(40) Davydov, R.; Kofman, V.; Nocek, J.; Noble, R. W.; Hui, H.; Hoffman, B. M. *Biochemistry* **2004**, *43*, 6330–6338.

Table 3. Decay of Hydroperoxoferri-P450cam–Substrate Complexes at 180 K: WT and T252A Mutant^a

substrate		WT (rel) ^b	T252A (rel) ^b
substrate-free	τ^a	<0.5	
camphor (a)	f_i	0.6	0.7 (1.1)
	τ_f	5.5 (1.0)	6.9 (1.2)
	τ_s	75	130 (1.7)
	$t_{1/2}^c$	8 (1)	8 (1.0)
5-methylenyl camphor (b)	f_i	0.3 (0.5)	0.6 (1)
	τ_f	6.0 (1.1)	93 (16)
	τ_s	120 (1.6)	1660 (22)
	$t_{1/2}^c$	40 (5.0)	140 (18)
5-F ₂ -camphor (c)	f_i	0.6 (1.0)	
	τ_f	5.9 (1.1)	
	τ_s	77 (1.0)	
	$t_{1/2}^c$	8 (1.0)	
norcamphor (d)	t	10 (1.8)	
	$t_{1/2}^c$	7 (0.9)	
adamantanone (e)	f_i	0.54 (0.9)	
	τ_f	3.8 (0.7)	
	τ_s	140 (1.9)	
	$t_{1/2}^c$	8 (1.0)	

^a Time in minutes; decay function, $I/I_0 = f_i \exp(-t/\tau_f) + (1 - f_i) \exp(-t/\tau_s)$; unless only one τ is given. Samples prepared with 40/60 (v/v) ethylene glycol/buffer as described in the Experimental Procedures. ^b Values relative to those for WT enzyme with camphor. ^c Defined as $I(t_{1/2})/I_0 = 1/2$.

similar (Figure 5); relaxation of **2**(T252A)-**b** decreases the value of A_{\max} , the value of 10.6 MHz seen for **2-a**, **b** (Table 2).

The ν_+ branch of the g_1 ¹⁴N ENDOR spectrum of as-formed **2**(T252A)-**b** again is complicated (Figure 4), being slightly more like that of **2-a** than **2-b**. However, relaxation at 170 K for 1 min simplifies the **2**(T252A)-**b** spectrum to one that is dominated by two quadrupole doublets (Table S1), as with **2-b** (Figure 4).

During prolonged annealing at 180 K, **2**(T252A)-**b** decays to ferriheme species with g_1 –2.51 and 2.43; the first of these may be a product state, while the second is the aquo-ferriheme state.⁴¹ GC-MS analysis shows that this decay is accompanied by stereospecific epoxidation of **b** with ~6% of total enzyme forming epoxide; again, ~80% of enzyme in the oxyferrous form, less than 50% forms **2**(252A)-**b**, and thus at least 14% of this intermediate generates product. Proton ENDOR discloses the presence of strongly coupled exchangeable protons, which indicates that this signal is not a ferriheme product state in which epoxide is complexed to the heme. ENDOR studies that employ isotopically labeled **b** will test whether this state is the primary product complex that contains an aquoferriheme and epoxide product, as is expected¹⁷ if **b** is epoxidized by the hydroperoxo-ferriheme rather than by compound I.

Decay Kinetics. We have monitored the decay kinetics of the relaxed hydroperoxo species, **2**, at 180 K. This has been done for the substrate-free WT enzyme and its complexes with **a–d**; for the mutant enzyme, it has been done with the **a** and **b** complexes. The WT, substrate-free **2** decays completely within 1 min at 180 K, implying a decay half-time of $t_{1/2} < 0.5$ min, which is too rapid for measurement. The presence of any substrate dramatically stabilizes **2**, and decay time-courses could be measured for every complex. In all complexes except for **2-e**, the decays are biphasic, presumably reflecting the existence of two substates of the distal heme pocket. Table 3 collects the ($1/e$) decay times for the two kinetic phases (τ_f ; τ_s) and the fraction of the faster phase (f_i). The fate of the $[\text{FeO}_2\text{H}]^7$ intermediate may depend on a competition between alternate processes—H₂O₂ loss versus reaction with substrate, versus formation of compound I—and the outcome of this competition

would change as the lifetime of the intermediate changes. Therefore, Table 3 also includes $t_{1/2}$ for each complex.

In all cases, τ_f for a complex of **2** or **2**(T252A) with a substrate is no less than 8–10-fold longer than the decay time for substrate-free **2**, and τ_s is at least another factor of 10 longer; the two phases typically have roughly equal weights (f_i), but this varies. However, these variations have negligible consequence in that they leave $t_{1/2} \approx 8$ min for all substrates but one: **a** and **c–e**, but not **b** (Table 3); the T252A mutation also leaves the decay half-time for **a** unchanged, $t_{1/2} = 8$ min, although it changes the individual decay parameters (Table 3).

The behavior of **2-b** is different. The value of τ_f of the **2-b** complex is the same as for **2-a**, while τ_s is slightly increased in **2-b**; however, f_i of **2-b** is half that of **2-a**. The result is that $t_{1/2}$ is 5-fold longer for the **2-b** intermediate: $t_{1/2} = 40$ min. The T252A mutation acts to further enable the perturbations of the heme pocket by **b**: replacing **a** with **b** as substrate in **2**(T252A) causes an additional 3-fold increase in $t_{1/2}$, to $t_{1/2} = 140$ min.

Discussion

We first discuss the structure of oxy-P450cam as indicated by the properties of intermediates **1** and **2** as-formed by cryoreduction. Then we discuss the relaxed **2**, which is an active hydroperoxo-ferriheme form in the sense that upon minimal further warming it continues along the catalytic pathway to product. We have examined the product states trapped after reaction of **2-a**, **2-b**, and **2**(T252A)-**b** and next discuss these findings. We further consider the implications of the measurements of the 180 K reaction/decay of the relaxed states of **2**. Finally, we describe a role of substrate in inducing the reactivity of an enzyme.

Oxy-P450cam. The species formed by cryoreduction of an oxyheme at 77 K retain the conformation of the oxyferrous-heme precursor, essentially unaltered. As a result, 77 K-reduced oxyferrous-P450 complexes provide an EPR/ENDOR probe of the active-site structure of the EPR-silent precursor oxyferrous-hemoprotein; in particular, if the product of reduction exhibits multiple EPR-active forms, the parent can be inferred to exist in multiple substates.^{13,17,28} EPR spectra (Figure 3; Table 1) show that all the samples studied except WT oxyferrous-P450-**d** and oxyferrous-P450(T252A)-**a** give rise to more than one reduced oxyferroheme species upon 77 K reduction, exhibiting signals from **1** and **2** and/or multiple forms of **2**. Therefore, with those exceptions, the active sites of all the oxyferrous-P450cam and oxyferrous-P450cam(T252A) complexes with substrate exist in multiple substates. This finding correlates with IR studies on CO-P450cam⁴² and recalls our recent report that the oxyferrous-heme centers of both the hemoglobin α and β chains and myoglobin exist in two substates.⁴⁰ The influence of substrate on the oxyferrous-heme conformation of oxyferrous-P450cam is modified by the T252A mutation. Thus, upon cryoreduction of oxyferrous-P450cam(T252A)-**a**, only the **2**(T252A)-**a** intermediate is trapped, while several species are formed with WT enzyme (Table 1 and Figure 3).

The g tensors of the as-formed reduced oxyferrous-heme centers provide a measure of their structure. The as-formed, substrate-free **2** has a g tensor with an unusually large value of

(41) Some conversion occurs during the 170 K relaxation, as well.

(42) Jung, C.; Hoa, G. H. B.; Schroeder, K. L.; Simon, M.; Doucet, J. P. *Biochemistry* **1992**, *31*, 12855–12862.

g_1 (Table 2), similar to that seen for HO,⁴³ which also does not have an additional substrate. The structure of an oxy-HO⁴⁴ shows that the Fe–O–O angle is unusually acute (110°), and this likely is true here as well. In the case of HO, this is because of steric constraints by residues of the distal pocket; that explanation cannot apply here. The g tensors of all the as-formed substrate complexes of **2** and **2**(T252A) are typical of hydroperoxoferriheme centers and vary only slightly among themselves. These observations suggest that the presence of a substrate allows the more normal Fe–O–O angle observed in the structure of oxy-P450cam-**a**,¹⁶ but why this is so is not obvious.

The higher resolution of ¹⁴N and ¹H ENDOR, relative to EPR, was used to probe the structure of oxy-P450cam through examination of the as-formed hydroperoxo-ferrihemes; the EPR spectrum of as-formed **1**, which represents the other major substate, is overlapped by that of **2** and could not be studied cleanly.

The ν_+ branch of the ¹⁴N spectrum of substrate-free **2**, both as-formed and after relaxation, shows a simple three-line pattern assigned to the overlap of quadrupole-split doublets from the two pairs of pyrrole ¹⁴N of a single well-defined substate (**eq 2**). In contrast, most of the substrate complexes of **2** and **2**(T252A) show more complex ¹⁴N patterns, which indicates that they are comprised of multiple second-tier substates with differing heme conformations; the spectrum of **2-b** most closely resembles the simple pattern of substrate-free enzyme. Differences in ¹⁴N patterns among these complexes indicate that the heme conformation is modulated by the substrate. The T252A mutation has minimal influence on the heme conformation of either **2-a** or **2-b**, presumably because the mutation occurs rather far from the heme.

The values of A_{\max} for the hydroperoxo proton of (**2**) and its substrate complexes reflect the bonding/conformation of the Fe–O–O–H moiety. The values of A_{\max} for as-formed **2** and the as-formed substrate complexes of **2** and **2**(T252A) exhibit a range of values, $9.9 \lesssim A_{\max} \lesssim 14.3$ MHz.

These indications that the conformation of the oxyferrous-heme center of substrate-free oxyferrous-P450cam differs from that in all the substrate complexes correlates with IR and RR studies on the substrate effect of the CO and NO complexes with ferrous P450cam.^{21,42} This difference between substrate-free and bound oxy-P450cam likely correlates with the stabilizing effect of substrate on oxy P450cam, and with the strong influence of **a–c** on the rates of NADH consumption during the monooxygenase cycle.³⁹ Although not of central focus in this paper, the assignment of the $g_1 \leq 2.25$ intermediate (**1**) as the peroxo-ferric intermediate [FeO₂],⁷ rather than a conformational variant of the [FeO₂H]⁷ form, is supported by the observation of a solvent kinetic isotope effect on its conversion to the hydroperoxo-ferric intermediate (**2**), as seen in the H/D difference in the relative amounts of **1-a** and **2-a** formed during 77 K cryoreduction (Figure 3).

Relaxed (Active) Hydroperoxo-ferric P450cam. Annealing cryoreduced samples to ca. 170 K relaxes the reduced heme center to the single, relaxed species **2**. The spectroscopic properties of relaxed substrate-free **2** again are distinctly different

from those of all substrate-bound relaxed **2**. Among these, **2-b** stands out as having the sharpest signal of any substrate complex of **2**. The T252A mutation does not significantly alter the g values of the **2-a,b** complexes.

In general, the ¹⁴N ENDOR spectra of the relaxed substrate complexes of **2** exhibit a limited simplification, indicating a lesser range of substate conformations; **2-b** stands out as exhibiting the simple overlap of doublets from a single substate, much like that of as-formed **2**, while the spectrum of **2**(T252A)-**b** is almost as well resolved (Figure 3). The ¹⁴N ENDOR data shows that the T252A mutation has essentially no influence on the heme conformation of **2-a**, **2-b** but does modulate that of **2b** somewhat. Presumably, the effects are small because the mutation occurs rather far from the heme.

For substrate complexes of **2**, with one exception, the range of ¹H couplings to the hydroperoxo proton is somewhat narrowed and shifted upon relaxation at 170 K, with $9 \lesssim A_{\max} \lesssim 11.5$ MHz. The exception again is **2-b**, where the hyperfine coupling is uniquely small: $A_{\max} = 7.5$ MHz. The full hyperfine tensor has been obtained for this species and is even more unusual (Table 2).

Enzymatic Primary Product States. In our original discussion of the mechanism of hydroxylation of **a** by P450cam, we identified the catalytically active species for the hydroxylation of camphor through proton ENDOR measurements on the primary product state.¹⁷ This state was shown to contain a ferriheme complexed with the oxygenated product, which implies that the catalytically active species is compound I; if it had contained an aqua-ferriheme complex, this would have implied that the hydroperoxo-ferriheme is catalytically active. By the same analysis, the absence of strongly coupled exchangeable protons in the primary product state formed upon epoxidation of **b** by the WT enzyme indicates that the epoxide produced binds to the ferriheme, or in some way protects it from binding H₂O, and thus identifies compound I as the intermediate that epoxidizes **b**. The presence of such protons in the putative primary product state formed upon epoxidation of **b** by P450cam(T252A) is compatible with recent conclusions⁸ that the reactive species in the mutant is the hydroperoxoferric state.

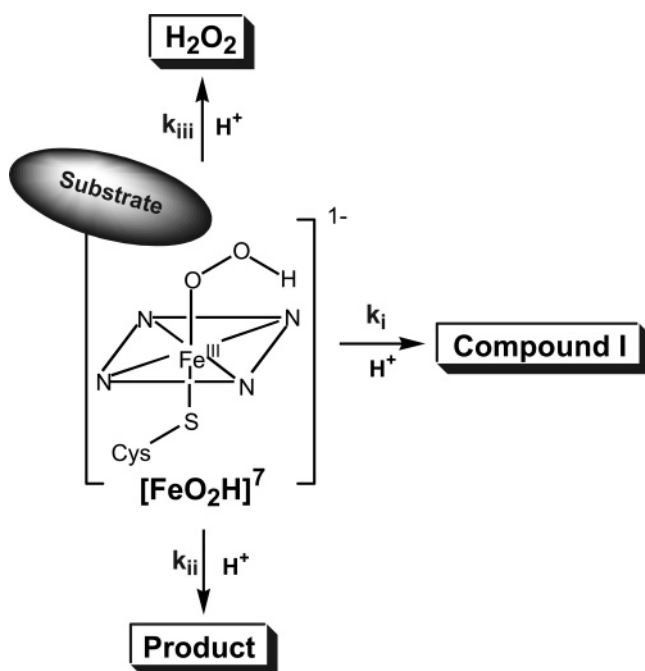
180K Reaction/Decay of Relaxed Hydroperoxo-ferric-P450 States. The presence of a substrate dramatically stabilizes hydroperoxoferri-P450cam. Viewed in terms of $t_{1/2}$, the complexes of **2** with all substrates except for **b** behave similarly, with $t_{1/2}$ more than 20-fold greater than that for substrate-free **2**. Remarkably, the most easily oxygenated substrate, **b**, further increases $t_{1/2}$ 5-fold. Nonetheless, the ¹H ENDOR data on the primary product complexes confirm that both **2-a** and **2-b** convert to compound I, which reacts with substrate to form product.

Looked at in more detail, all the substrate complexes of **2** and **2**(T252A) show biphasic decay at 180 K, except for **2-d**, and the more rapidly decaying phase lives at least 10-fold longer than substrate-free **2**; the more slowly decaying phase lives at least 100 times longer (Table 3). This biphasic decay is seen for intermediates that have a well-defined EPR spectrum and thus exist in one major (first-tier) substate. Therefore, the two-phase reactivity of this intermediate is indicative that the overall active site, defined to include the distal-pocket proton delivery network, and not the heme alone, exists in (at least) two substates

(43) Davydov, R. M.; Yoshida, T.; Ikeda-Saito, M.; Hoffman, B. M. *J. Am. Chem. Soc.* **1999**, *121*, 10656–10657.

(44) Unno, M.; Matsui, T.; Chu, G. C.; Couture, M.; Yoshida, T.; Rousseau, D. L.; Olson, J. S.; Ikeda-Saito, M. *J. Biol. Chem.* **2004**, *279*, 21055–21061.

Scheme 2



with different decay times and that they are noninterconverting, or slowly interconverting, at 180 K. The suggestion that the source of the biphasic decay at 180 K is located within the proton delivery system, not at the heme, is supported by the finding that the EPR/ $^{14}\text{N}/^1\text{H}$ ENDOR data show that the properties of the hydroperoxo-ferriheme are modified by the substrate, yet its decay kinetics are largely insensitive to these perturbations at the heme (Table 3), except for **2**(T252A)-**b**. Specifically, we suggest that the rate-limiting step in this decay involves transfer of a proton to the $-\text{OOH}$ moiety, as is the case for heme oxygenase.¹⁴

It is noteworthy that $t_{1/2}$ is the same for **2**(T252A)-**a** as for **2**-**a**, given that **2**(T252A)-**a** loses H_2O_2 rather than forming compound I. This can be illustrated with Scheme 2. There are three channels by which **2** can react: (i) to compound I; (ii) direct to product; and (iii) to the ferriheme state with release of H_2O_2 . For the intermediates **2**-**a**, and almost certainly, **2**-**b**, the rates have the relation $k_i \gg (k_{ii} + k_{iii})$: compound I is formed almost exclusively and is the reactive intermediate. The T252A mutation does not change $t_{1/2}$ of **2**(T252A)-**a** from that of **2**-**a** and yet changes its fate to the release of H_2O_2 . In terms of the kinetic scheme for decay of **2**, this means that with **a** as the substrate, the mutation drastically decreases k_i (T252A) while increasing k_{iii} (T252A), such that k_{iii} (T252A) $\approx k_i$ (WT) $\gg (k_i$ (T252A) + k_{ii} (T252A)).

The change of substrate from **a** to **b** in **2**(T252A) causes an additional 3-fold increase in $t_{1/2}$, and this is accompanied by a change in the fate of the hydroperoxo-ferric heme: in **2**(252A)-**a** ($t_{1/2} = 8$ min), it accepts a proton and releases H_2O_2 ; in **2**(T252A)-**b** ($t_{1/2} = 140$ min), it proceeds to the epoxide product. Within the kinetic scheme, this means that the alternate substrate reduces k_{iii} by far more than a factor of 20 such that now $k_{iii} \ll (k_i + k_{ii}) \approx (190 \text{ min})^{-1}$ (Scheme 2). In the original report of this phenomenon,⁸ it was suggested that **2**(T252A)-**b** may be reacting directly to form epoxide rather than forming compound I as the catalytically active intermediate. This would mean that the joint influence of the substrate/mutation has slowed the loss

of H_2O_2 enough (18-fold increase in $t_{1/2}$) that the reaction of the $[\text{FeO}_2\text{H}]^7$ intermediate with substrate has become kinetically competitive with H_2O_2 loss, namely, that now $k_i \ll k_{ii} \approx (140 \text{ min})^{-1}$. Indeed, the limited ^1H ENDOR data presented here for the putative product complex is compatible with this suggestion.

However, the present kinetic results suggest that we should reexamine this idea, as they call into question the expectation on which it was based, namely, that if compound I is not formed from **2**(T252A) when **a** is the substrate, then it is not formed when **b** is the substrate. With the extended lifetime of **2**(T252A)-**b**, it could equally well be that the rate of loss of H_2O_2 (k_{iii}) has been greatly lessened such that $k_{iii} \ll (k_i + k_{ii})$, and H_2O_2 loss no longer dominates the reaction, but that the slow formation of compound I nonetheless remains kinetically competitive with direct reaction, $k_{ii} \ll k_i \approx (190 \text{ min})^{-1}$; thus, with **b** as substrate in P450cam(T252A), the reactive intermediate might nonetheless be compound I.

Conclusions

The present study shows that the properties and reactivity of one-electron reduced intermediates of oxy-P450cam can be modulated by a bound substrate. These influences include direct alterations in the properties of the heme center (g tensor; ^{14}N , ^1H hyperfine couplings) upon incorporation of the substrate. However, they also include perturbations of the distal-pocket proton delivery, as manifest in changes in reactivity: the presence of any substrate dramatically stabilizes hydroperoxo-ferri-P450cam, with substrate complexes of **2** (hydroperoxo-ferri-P450cam) living no less than ca. 20 times longer than substrate-free **2**.

Among the substrates, **b** (Chart 1) stands out as having an exceptionally strong influence on the properties of the P450cam intermediates, presumably because of the extra steric bulk of the $(=\text{CH}_2)$ group at the site of reaction. The EPR spectra of **2**-**b** are uniquely sharp; the g values are unusual, and the hyperfine coupling to the hydroperoxo proton is unusually small, suggesting an altered $(-\text{OOH})$ conformation. The ^{14}N ENDOR spectra of as-formed and relaxed **2**-**b** and **2**(T252A)-**b** are unique among substrate complexes of **2** in disclosing a single major heme conformational substate. The substrate **b** also stands alone in changing reactivity as well as structure. In the wt enzyme, all relaxed **2**-substrate complexes studied exhibit the same decay time, $t_{1/2} \sim 8$ min, at 180 K, except for **2**-**b**, whose $t_{1/2}$ is 5-fold longer. The T252A mutation leaves $t_{1/2}$ unchanged when **a** is substrate, but $t_{1/2} = 140$ min for **2**(T252A)-**b**, 3-fold greater than that of **2**-**b**. This combination of substrate/mutation-induced effects of **b** alters the fate of **2**(T252A)-**b**. Rather than nonproductively losing H_2O_2 , as occurs with **2**(T252)-**a**, the **2**(T252)-**b** intermediate decays with formation of the epoxide of **b**. The change in pathway may also involve a change in the reactive intermediate, with **2**(T252A)-**b** reacting to form product without formation of compound I. But the difference in the lifetimes of **2**(252)-**a** and **2**(T252A)-**b** calls into question the arguments to this effect. Further mechanistic and spectroscopic measurements will be required to resolve this issue; the study of other substrates with varying steric bulk at the 5-position of camphor also is indicated.

The view that emerges from this discussion is that a substrate does not react within an active site: the active site is the protein and its prosthetic group(s) plus the substrate. In an extension

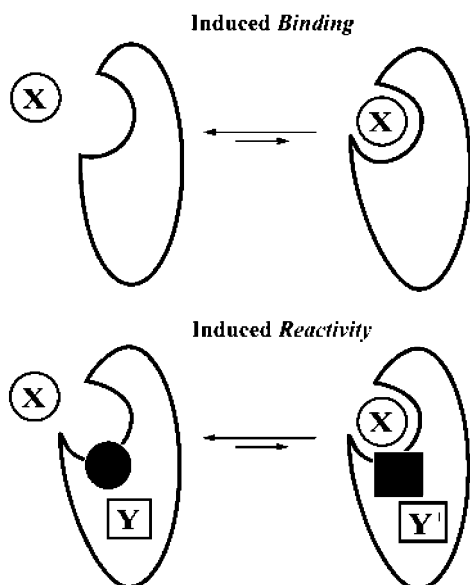


Figure 7. Schematic representation of substrate-induced binding (upper) and reactivity (lower).

of the well-established idea of induced-fit for substrate binding⁴⁵ (Figure 7) so must one consider induced reactivity in which substrate modulates the properties of a reactive intermediate,

taking catalytic element(s) **Y** to perturbed form(s), **Y'**; in monooxygenase enzymes this means a modulation of both the properties of the active-oxygen heme intermediates and the proton-delivery network that encompasses them. We surmise that such modulation of the reactivity of an enzyme intermediate by its substrate may play a significant role in determining the monooxygenase enzyme's mechanism in other instances and may explain the proposed presence of multiple oxidants and multiple mechanisms as cyt P450 reacts with different substrates.^{7,46}

Acknowledgment. We thank NIH support (HL13531, B.M.H.; GM 26730, J.H.D.); Prof. H. Halpern, Pritzker School of Medicine, University of Chicago, for access to the ⁶⁰Co irradiator; and Prof. Stephen G. Sligar, Department of Biochemistry, University of Illinois, for the P450cam (T252A) overexpression system.

Supporting Information Available: Table of ¹⁴N spin-Hamiltonian parameters (Table S1). This material is available free of charge via the Internet at <http://pubs.acs.org>.

JA045351I

- (45) Koshland, D. E., Jr.; Nemethy, G.; Filmer, D. *Biochemistry* **1966**, *5*, 365–385.
 (46) Vaz, A. D. N.; McGinness, D. F.; Coon, M. J. *Proc. Natl. Acad. Sci. U.S.A.* **1998**, *95*, 3555–3560.